Acta Crystallographica Section F
Structural Biology and Crystallization Communications
ISSN 1744-3091

Cloning, expression, purification, crystallization and preliminary X-ray diffraction analysis of glyoxalase I from *Leishmania infantum*

Lídia Barata,[a,b] Marta Sousa Silva,[a,c] Linda Schuldt,[b] Gonçalo da Costa,[a] Ana M. Tomás,[c,d] António E. N. Ferreira,[a] Manfred S. Weiss,[b]‡ Ana Ponces Freire[a] and Carlos Cordeiro[a]*

[a]Centro de Química e Bioquímica, Departamento de Química e Bioquímica, Faculdade de Ciências, Universidade de Lisboa, Lisboa, Campo Grande, Edifício C8, 1149-016 Lisboa, Portugal, [b]European Molecular Biology Laboratory, Hamburg Outstation, c/o DESY, Notkestrasse 85, D-22603 Hamburg, Germany, [c]IBMC, Instituto de Biologia Molecular e Celular, Universidade do Porto, Rua do Campo Alegre 823, 4150-180 Porto, Portugal, and [d]ICBAS, Instituto de Ciências Biomédicas Abel Salazar, Universidade do Porto, Largo Professor Abel Salazar 2, 4099-003 Porto, Portugal

‡ Present address: Helmholtz-Zentrum Berlin für Materialien und Energie, Macromolecular Crystallography (BESSY-MX), Albert-Einstein-Strasse 15, D-12489 Berlin, Germany.

Correspondence e-mail: caac@fc.ul.pt

Received 9 October 2009
Accepted 22 March 2010

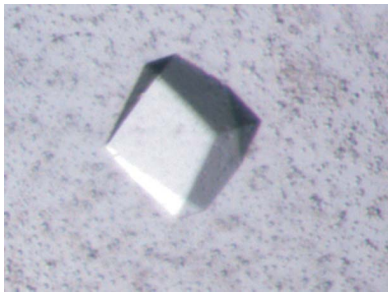

Glyoxalase I (GLO1) is the first of the two glyoxalase-pathway enzymes. It catalyzes the formation of *S*-D-lactoyltrypanothione from the non-enzymatically formed hemithioacetal of methylglyoxal and reduced trypanothione. In order to understand its substrate binding and catalytic mechanism, GLO1 from *Leishmania infantum* was cloned, overexpressed in *Escherichia coli*, purified and crystallized. Two crystal forms were obtained: a cube-shaped form and a rod-shaped form. While the cube-shaped form did not diffract X-rays at all, the rod-shaped form exhibited diffraction to about 2.0 Å resolution. The crystals belonged to space group $P2_12_12$, with unit-cell parameters $a = 130.03$, $b = 148.51$, $c = 50.63$ Å and three dimers of the enzyme per asymmetric unit.

1. Introduction

Trypanosomatids are the causative agents of leishmaniasis, a group of diseases that are widespread in the Third World and the Mediterranean Basin and that affect nearly 12 million people according to the World Health Organization. Effective therapeutic approaches for leishmaniasis may rely on unique biochemical characteristics that set trypanosomatids apart from other eukaryotic cells. Two of these features are the compartmentalization of glycolysis into a specific organelle, the glycosome (Michels *et al.*, 2000; Hannaert *et al.*, 2003), and the functional replacement of glutathione by trypanothione [N^1,N^8-bis(glutathionyl)spermidine], a spermidine–glutathione conjugate (Müller *et al.*, 2003; Flohé *et al.*, 1999). By synergistically exploiting the disruption of trypanothione-dependent biochemical processes and the inhibition of the glycolytic pathway (Bakker *et al.*, 1999), both of which are essential for parasite survival, new therapeutic targets may be identified. One of these trypanothione-dependent systems is the glyoxalase pathway, which is responsible for the elimination of methylglyoxal, a toxic and mutagenic compound (Thornalley, 1998) that originates from either spontaneous degradation of triose phosphates or a side reaction of triphosphate isomerase.

In trypanosomatids, the methylglyoxal elimination system is composed of two enzymes (Fig. 1): glyoxalase I (lactoylglutathione lyase; EC 4.4.1.5; GLO1) and glyoxalase II (hydroxyacylglutathione hydrolase; EC 3.1.2.6; GLO2). These enzymes are specific for trypanothione and lactoyltrypanothione, respectively (Sousa Silva *et al.*, 2005; Irsch & Krauth-Siegel, 2004), although GLO1 also catalyses the reaction of the glutathione–methylglyoxal hemithioacetal (Sousa Silva *et al.*, 2005).

In eukaryotes, GLO1 is a homodimeric protein consisting of two subunits of 141 residues each (molecular weight 18.2 kDa). In prokaryotes the enzyme is also dimeric (Sukdeo *et al.*, 2004), while in yeast (Thornalley, 2003) and plasmodia (Iozef *et al.*, 2003) the enzyme is monomeric, although two genes for the enzyme exist owing to a gene-duplication event. The relative size and structure of the enzyme is conserved across all of the above organisms. X-ray structures of GLO1 from various organisms are known, including the enzymes from *Escherichia coli* (*Ec*GLO1; PDB entries 1f9z, 1fa5, 1fa6, 1fa7 and 1fa8; He *et al.*, 2000), *Homo sapiens* (*Hs*GLO1; PDB entries 1fro, 1qin, 1qip and 1bh5; Cameron *et al.*, 1997, 1999; Ridderstrom *et al.*, 1998) and *Leishmania major* (*Lm*GLO1; PDB entry 2c21; Ariza *et al.*,

2006). All of these structures display a homodimeric arrangement of the molecules.

Although *Lm*GLO1 shows 97% sequence identity to the enzyme from *L. infantum* (*Li*GLO1), the forms of leishmaniasis caused by the two organisms are very different. This may be attributed to differences in stage-regulated gene-expression patterns between *L. infantum* and *L. major* (Rochette *et al.*, 2008), but may also arise from amino-acid differences in the respective enzymes.

Here, we report the cloning, expression, purification, crystallization and preliminary X-ray diffraction analysis of *Li*GLO1. In addition, the structure of *Li*GLO1 was solved by molecular replacement. Together with the previously solved structure of *L. infantum* GLO2 (Silva *et al.*, 2008), the refined structure of *Li*GLO1 will lead to a better understanding of the glyoxalase pathway in trypanosomatids as well as providing novel insights into the evolutionary pressure towards trypanothione specificity.

2. Materials and methods

2.1. Cloning and expression

The *Li*GLO1 gene (GenBank accession No. DQ294973) was amplified from *L. infantum* genomic DNA. The PCR product was cloned [forward primer 5′-CCGCGCA**CATATG**CCGTCTCGTCG-TAT-3′, containing an *Nde*I restriction site (bold); reverse primer 5′-CACCG**CTCGAG**TTACGCAGTGCCCTGCTC-3′, containing an *Xho*I restriction site (bold) immediately after the stop codon] into the *Nde*I/*Xho*I-digested expression vector pET28a (Novagen, Gibbstown, USA), which was then transformed into *E. coli* BL21-CodonPlus (Stratagene, La Jolla, California, USA). The correct cloning of the open reading frame was confirmed by sequencing. The final protein sequence was preceded by MGSS**HHHHHH**SSG*LVPRGS*H, containing a His_6 tag (bold) and a thrombin cleavage site (italics). For overexpression of N-terminally His_6-tagged *Li*GLO1, *E. coli* BL21-CodonPlus transformants were grown in LB medium containing 50 µg ml^{-1} kanamycin and 34 µg ml^{-1} chloramphenicol at 310 K. Expression of His_6-tagged *Li*GLO1 was induced at a culture OD_{600} of 0.6 with 0.1 m*M* isopropyl *β*-D-1-thiogalactopyranoside (IPTG) for 3 h at 310 K. Cells were harvested by centrifugation at 7800*g* for 30 min at 277 K and the cell pellets were frozen at 253 K.

2.2. Purification

The cell pellet was suspended in 10 ml buffer *A* (50 m*M* bis-tris pH 6.3, 200 m*M* NaCl; all chemicals were obtained from Carl Roth, Karlsruhe, Germany) per gram of cells and lysed by sonication for 10 min at 35% power using 0.4 s pulses with 0.9 s breaks between the pulses at 277 K. The soluble fraction obtained by centrifugation at 38 000*g* for 40 min at 277 K was filtered through a 0.22 µm membrane before being applied onto an affinity-chromatography column charged with Co^{2+} for purification at room temperature. The fusion protein, which contained an N-terminal tail consisting of six histidine residues and a thrombin cleavage site, was eluted in buffer *A* supplemented with 500 m*M* imidazole. The N-terminal His_6 tag was cleaved using a Thrombin Cleavage Kit (Novagen) with optimized cleavage conditions (1:200 thrombin dilution overnight at 293 K). The cleaved protein was directly applied onto a gel-filtration column (Superdex S75 16/60, GE Healthcare) equilibrated with buffer *A* for further purification. The purity of the recombinant enzyme was estimated by SDS–PAGE. Peptide mass fingerprinting by MALDI-FTICR MS was used to confirm the identity of the expressed protein (Shevchenko *et al.*, 2006). *Li*GLO1 was concentrated to 15 mg ml^{-1} in buffer *A* using a Vivaspin 15 (molecular-weight cutoff 10 000) concentrator (Sartorius Stedim Biotech, Göttingen, Germany). The protein concentration was determined using a Peqlab Biotechnologie GmbH NanoDrop ND-1000 spectrometer at 280 nm, assuming an estimated *Li*GLO1 extinction coefficient of 20 400 M^{-1} cm^{-1} as calculated using the *ProtParam* tool (Gasteiger *et al.*, 2005) for a protein of molecular weight 18.2 kDa. Buffer *A* was optimized by ligand-assisted monitoring of thermal protein unfolding in a ThermoFluor (Bio-Rad, California, USA) experiment (data not shown).

2.3. Crystallization

Initial crystallization screening was performed at the High Throughput Crystallization facility at the EMBL Hamburg Outstation (Mueller-Dieckmann, 2006) using commercially available crystal screens and the sitting-drop vapour-diffusion method. The drops consisted of 0.5 µl protein solution at a concentration of 15 mg ml^{-1} and 0.5 µl reservoir solution and were equilibrated over 80 µl reservoir solution using 96-well format Greiner plates. Two crystal forms (Fig. 2) were obtained from two different crystallization conditions: conditions B1 [70%(*v*/*v*) 2-methyl-2,4-pentanediol (MPD), 100 m*M* MES sodium salt pH 6.5] and B2 [70%(*v*/*v*) MPD, 100 m*M* Tris–HCl

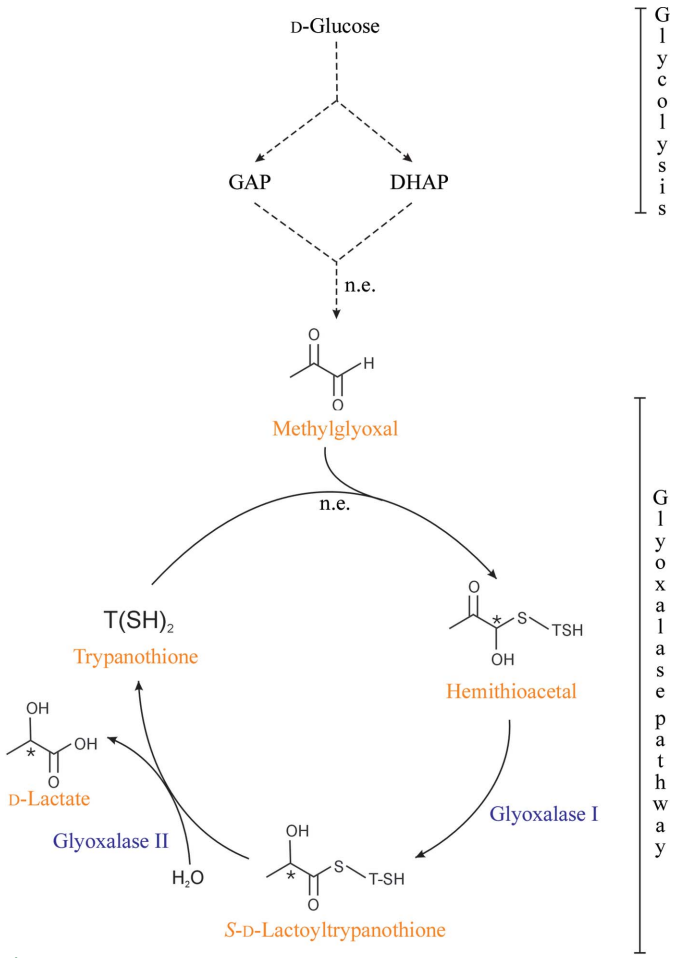

Figure 1
Metabolism of methylglyoxal in *Leishmania* spp. Methylglyoxal originates non-enzymatically (n.e.) from glyceraldehyde phosphate or dihydroxyacetone phosphate and is further catabolized in the glyoxalase pathway. Here, methylglyoxal reacts non-enzymatically with reduced trypanothione [$T(SH)_2$], forming a hemithioacetal. This hemithioacetal is then isomerized by GLO1, forming the thiol ester *S*-D-lactoyltrypanothione, which is subsequently hydrolysed to D-lactate by GLO2, regenerating $T(SH)_2$.

Table 1
Data-collection and processing statistics.

Values in parentheses are for the highest resolution shell.

Beamline	ID23-1, ESRF	X12, EMBL, DESY
Detector	ADSC Q315r	MAR CCD 225 mm
No. of crystals	1	1
Wavelength (Å)	0.8726	1.0000
Crystal-to-detector distance (mm)	360	200
Rotation range per image (°)	1.0	0.5
Total rotation range (°)	120	200
Resolution range (Å)	50.0–3.09 (3.27–3.09)	50.0–2.10 (2.20–2.10)
Space group	$P2_12_12$	$P2_12_12$
Unit-cell parameters		
a (Å)	130.60	130.03
b (Å)	149.01	148.51
c (Å)	50.40	50.63
Mosaicity (°)	0.231	0.116
Total No. of reflections	89612	474893
Unique reflections	18622	110729
Redundancy	4.8 (4.8)	4.3 (4.2)
$\langle I/\sigma(I)\rangle$	10.4 (2.2)	12.8 (2.2)
Completeness (%)	99.0 (95.7)	99.8 (98.9)
$R_{\rm merge}$† (%)	18.1 (77.2)	9.7 (77.8)
$R_{\rm r.i.m.}$‡ (%)	20.2 (86.8)	10.4 (83.1)
$R_{\rm p.i.m.}$§ (%)	8.9 (39.6)	3.6 (28.9)
Overall *B* factor from Wilson plot (Å^2)	71.7	32.3
Optical resolution (Å)	2.19	1.65

† $R_{\rm merge} = \sum_{hkl}\sum_i |I_i(hkl) - \langle I(hkl)\rangle|/\sum_{hkl}\sum_i I_i(hkl)$, where $I_i(hkl)$ is the intensity of observation i of reflection hkl. ‡ $R_{\rm r.i.m} = \sum_{hkl}[N/(N-1)]^{1/2}\sum_i |I_i(hkl) - \langle I(hkl)\rangle|/\sum_{hkl}\sum_i I_i(hkl)$, where $I_i(hkl)$ is the intensity of observation i of reflection hkl and N is the redundancy of reflection hkl. § $R_{\rm p.i.m} = \sum_{hkl}[1/(N-1)]^{1/2}\sum_i |I_i(hkl) - \langle I(hkl)\rangle|/\sum_{hkl}\sum_i I_i(hkl)$, where $I_i(hkl)$ is the intensity of observation i of reflection hkl and N is the redundancy of reflection hkl.

pH 8.5] of JBScreen Classic 8 from Jena Bioscience (Jena, Germany). Crystals of form 2 were then further improved by applying the hanging-drop vapour-diffusion method using the tools from Nextal Biotechnology (Montreal, Canada). Drops were prepared by mixing 2 µl protein solution with 2 µl reservoir solution consisting of 62%(*v*/*v*) MPD and 100 m*M* Tris–HCl pH 8.5 and were equilibrated over 1 ml reservoir solution. This resulted in rod-shaped crystals (Fig. 2*c*), which grew within 3 d at 293 K to maximum dimensions of 0.50 × 0.15 × 0.15 mm.

2.4. Diffraction data collection and processing

For diffraction experiments, the crystals were directly flash-cooled in the cryostream without any additional cryoprotectant. The cube-shaped crystals (Fig. 2*a*) did not show any X-ray diffraction on beamline ID23-2 at the European Synchrotron Research Facility (ESRF, Grenoble, France). However, the initial rod-shaped crystals from the second condition (Fig. 2*b*) diffracted to 3.0 Å resolution on the same beamline (Table 1) and a complete diffraction data set was collected. The optimized form 2 crystals diffracted to about 2.0 Å on EMBL beamline X12 [Deutsches Elektronen-Synchrotron (DESY), Hamburg, Germany]. Again, a complete diffraction data set was collected to 2.1 Å resolution (Table 1). All data were processed and scaled using *XDS* (Kabsch, 1993, 2010). The *R* factors $R_{\rm r.i.m.}$ (redundancy-independent merging *R* factor) and $R_{\rm p.i.m.}$ (precision-indicating merging *R* factor) (Weiss, 2001) were obtained using the program *RMERGE* (available from http://www.embl-hamburg.de/~msweiss/projects/msw_qual.html or from MSW upon request). The optical resolution was calculated using the program *SFCHECK* (Vaguine *et al.*, 1999) and the self-rotation function was calculated using the program *MOLREP* (Vagin & Teplyakov, 1997) for data between 99 and 4.0 Å resolution.

3. Results and discussion

After purification of *Li*GLO1 using cobalt affinity chromatography and a gel-filtration step, the protein was about 95% pure as estimated by SDS–PAGE. The total yield of the purification process was 20 mg of protein per litre of culture. The crystallization behaviour was observed to be similar to that of the enzyme from *L. major* (Ariza *et al.*, 2005). The initial rod-shaped form 2 crystals (Fig. 2*b*) diffracted to about 3.0 Å resolution, while the optimized crystals (Fig. 2*c*) diffracted X-rays to beyond 2.1 Å resolution using synchrotron radiation. Two complete diffraction data sets were collected (Table 1). The crystals belonged to space group $P2_12_12$, with unit-cell para-

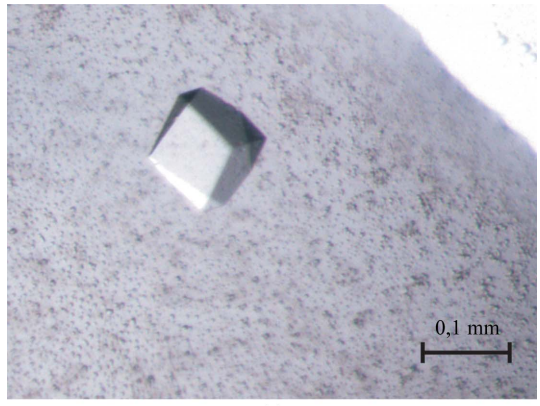

(*a*)

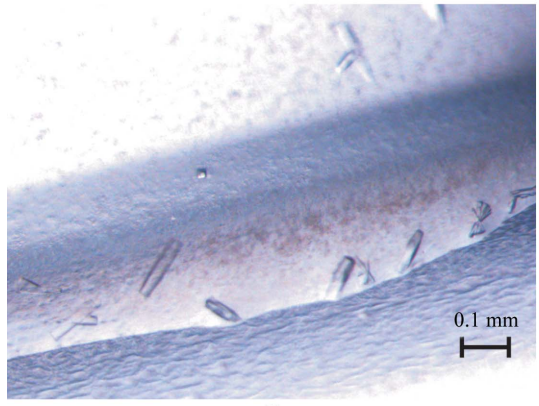

(*b*)

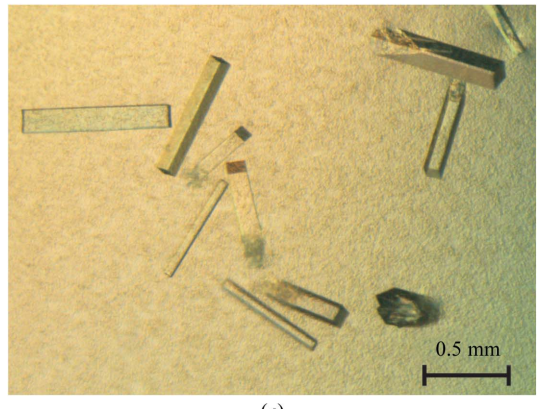

(*c*)

Figure 2
Crystals of *Li*GLO1. (*a*) Form 1 crystals with dimensions of approximately 0.1 × 0.1 × 0.1 mm. These crystals did not exhibit any diffraction in the X-ray beam. (*b*) Initial form 2 crystals with dimensions of approximately 0.15 × 0.03 × 0.03 mm. These crystals diffracted to about 3.0 Å resolution. (*c*) Improved form 2 crystals with dimensions of approximately 0.5 × 0.15 × 0.15 mm. These crystals diffracted to about 2.0 Å resolution.

meters a = 130.03, b = 148.51, c = 50.63 Å. The Matthews coefficient V_M (Matthews, 1968) and solvent content calculated based on a subunit molecular weight of 18.2 kDa (predicted from the sequence) estimated the most likely asymmetric unit content to be either four or six molecules. Assuming the presence of three dimers per asymmetric unit, the Matthews coefficient was 2.2 Å^3 Da^{-1} and the solvent content was 45.3% (Kantardjieff & Rupp, 2003; Matthews, 1968). For two dimers the respective values would be 3.4 Å^3 Da^{-1} and 63.6%. A detailed examination of the self-rotation function revealed noncrystallographic peaks on the $\kappa = 180^\circ$ section (Fig. 3). It appears to be the case that at least two additional twofold axes are present on this section and that all of them lie in the xy plane. However, without knowledge of the structure the self-rotation function does not allow determination of the number of dimers per asymmetric unit with certainty.

The structure of *Li*GLO1 was solved by molecular replacement using the related structure of glyoxalase I from *L. major* (PDB entry 2c21; Ariza *et al.*, 2006) and the lower resolution data set collected from the initial form 2 crystals. After placing three dimers in the asymmetric unit, the correlation coefficient was 64.2% and the R factor to 3.5 Å resolution was 39.6%. This essentially confirmed the correctness of the structure solution. Refinement of the structure against the high-resolution data set collected from the optimized form 2 crystals is currently under way. In retrospect, the self-rotation function (Fig. 3) can be examined and interpreted using the known structure as a guide. The three dimers of *Li*GLO1 arrange themselves in a pseudo-$D3$ symmetric arrangement, with the threefold axis only about 14° away from the crystallographic z axis and all twofold axes close to the xy plane. A very similar arrangement was also observed in the structure of *Lm*GLO1 (Ariza *et al.*, 2005).

Together with the previously determined structure of *L. infantum* GLO2 (Silva *et al.*, 2008), the *Li*GLO1 structure will not only allow a comprehensive study of the glyoxalase pathway in trypanosomatids but will also provide insight into the reasons for trypanothione selection during evolution.

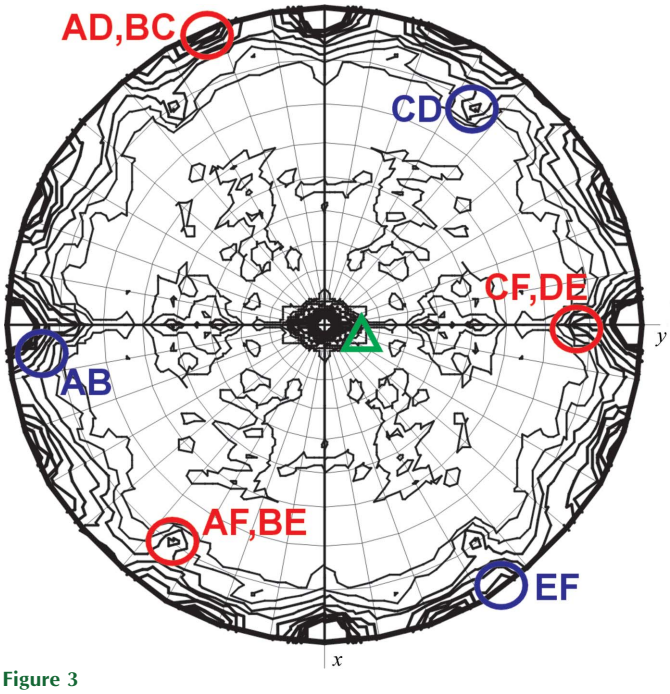

Figure 3
Self-rotation function of the *Li*GLO1 native data. The $\kappa = 180^\circ$ section is shown, indicating the relative locations of the twofold-symmetry axes. The peaks originating from the crystallographic symmetry are located along the x, y and z directions. The peaks representing the noncrystallographic symmetry elements are highlighted and labelled with the respective subunit identifiers. Blue circles show the twofold axes relating the two monomers within one *Li*GLO1 dimer and red circles show the twofold axes relating the monomers of different dimers to each other. In addition, the position of the noncrystallographic threefold axis is indicated by a green triangle (note: the peak corresponding to the green triangle does of course not appear on the $\kappa = 180^\circ$ section depicted here but instead appears on the $\kappa = 120^\circ$ section). The three dimers of *Li*GLO1 in the asymmetric unit assemble into a hexamer of approximate $D3$ symmetry. This figure was produced using the program *MOLREP* (Vagin & Teplyakov, 1997).

The authors acknowledge the European Synchrotron Research Facility (ESRF, Grenoble, France) and EMBL Hamburg at the Deutsches Elektronen-Synchrotron (DESY, Hamburg, Germany) for access to synchrotron beamtime. The work was supported by projects POCTI/ESP/48272/2002, POCI/QUI/62027/2004 and REDE/1501/REM/2005 (Fundação para a Ciência e Tecnologia, Portugal). LB was supported by doctoral grant SFRH/BD/28691/2006 from Fundação para a Ciência e Tecnologia (Portugal) and by EMBO short-term fellowship ASTF 318-2008.

References

Ariza, A., Vickers, T. J., Greig, N., Armour, K. A., Dixon, M. J., Eggleston, I. M., Fairlamb, A. H. & Bond, C. S. (2006). *Mol. Microbiol.* **59**, 1239–1248.
Ariza, A., Vickers, T. J., Greig, N., Fairlamb, A. H. & Bond, C. S. (2005). *Acta Cryst.* F**61**, 769–772.
Bakker, B. M., Walsh, M. C., ter Kuile, B. H., Mensonides, F. I., Michels, P. A., Opperdoes, F. R. & Westerhoff, H. V. (1999). *Proc. Natl Acad. Sci. USA*, **96**, 10098–10103.
Cameron, A. D., Olin, B., Ridderstrom, M., Mannervik, B. & Jones, T. A. (1997). *EMBO J.* **16**, 3386–3395.
Cameron, A. D., Ridderstrom, M., Olin, B., Kavarana, M. J., Creighton, D. J. & Mannervik, B. (1999). *Biochemistry*, **38**, 13480–13490.
Flohé, L., Hecht, H.-J. & Steinert, P. (1999). *Free Radic. Biol. Med.* **27**, 966–984.
Gasteiger, E., Hoogland, C., Gattiker, A., Duvaud, S., Wilkins, M. R., Appel, R. D. & Bairoch, A. (2005). *The Proteomics Protocols Handbook.* Totowa: Humana Press.
Hannaert, V., Bringaud, F., Opperdoes, F. R. & Michels, P. A. (2003). *Kinetoplastid Biol. Dis.* **2**, 11.
He, M. M., Clugston, S. L., Honek, J. F. & Matthews, B. W. (2000). *Biochemistry*, **39**, 8719–8727.
Iozef, R., Rahlfs, S., Chang, T., Schirmer, H. & Becker, K. (2003). *FEBS Lett.* **554**, 284–288.
Irsch, T. & Krauth-Siegel, R. L. (2004). *J. Biol. Chem.* **279**, 22209–22217.
Kabsch, W. (1993). *J. Appl. Cryst.* **26**, 795–800.
Kabsch, W. (2010). *Acta Cryst.* D**66**, 125–132.
Kantardjieff, K. A. & Rupp, B. (2003). *Protein Sci.* **12**, 1865–1871.
Matthews, B. W. (1968). *J. Mol. Biol.* **33**, 491–497.
Michels, P. A., Hannaert, V. & Bringaud, F. (2000). *Parasitol. Today*, **16**, 482–489.
Müller, S., Liebau, E., Walter, R. D. & Krauth-Siegel, R. L. (2003). *Trends Parasitol.* **19**, 320–328.
Mueller-Dieckmann, J. (2006). *Acta Cryst.* D**62**, 1446–1452.
Ridderstrom, M., Cameron, A. D., Jones, T. A. & Mannervik, B. (1998). *J. Biol. Chem.* **273**, 21623–21628.
Rochette, A., Raymond, F., Ubeda, J. M., Smith, M., Messier, N., Boisvert, S., Rigault, P., Corbeil, J., Ouellette, M. & Papadopoulou, B. (2008). *BMC Genomics*, **9**, 255.
Silva, M. S., Barata, L., Ferreira, A. E., Romao, S., Tomás, A. M., Freire, A. P. & Cordeiro, C. (2008). *Biochemistry*, **47**, 195–204.
Sousa Silva, M., Ferreira, A. E., Tomás, A. M., Cordeiro, C. & Ponces Freire, A. (2005). *FEBS J.* **272**, 2388–2398.
Shevchenko, A., Tomás, H., Havlis, J., Olsen, J. V. & Mann, M. (2006). *Nature Methods*, **1**, 2856–2860.
Sukdeo, N., Clugston, S. L., Daub, E. & Honek, J. F. (2004). *Biochem. J.* **384**, 111–117.
Thornalley, P. J. (1998). *Chem. Biol. Interact.* **111–112**, 137–151.
Thornalley, P. J. (2003). *Biochem. Soc. Trans.* **31**, 1343–1348.
Vagin, A. & Teplyakov, A. (1997). *J. Appl. Cryst.* **30**, 1022–1025.
Vaguine, A. A., Richelle, J. & Wodak, S. J. (1999). *Acta Cryst.* D**55**, 191–205.
Weiss, M. S. (2001). *J. Appl. Cryst.* **34**, 130–135.